Analysis of the photon indistinguishability in incoherently excited quantum dots

F. Troiani,* J. I. Perea, and C. Tejedor
Departamento de Fisica Teorica de la Materia Condensada, Universidad Autonoma de Madrid, 28049 Madrid, Spain
(Received 14 October 2005; revised manuscript received 30 November 2005; published 17 January 2006)

The solid-state single-photon sources so far demonstrated require energy relaxation processes, which tend to spoil the coherent nature of the time evolution and with it the photon indistinguishability. We focus our theoretical investigation on semiconductor quantum dots embedded in microcavities. In the slow-dephasing limit, the photon indistinguishability is shown to decrease with the ratio between nonradiative and radiative emission rates, according to a simple analytical relation. The effect of dephasing is then investigated within a wide range of physical parameters, providing clear indications for the device optimization.

DOI: 10.1103/PhysRevB.73.035316 PACS number(s): 03.67.Lx, 42.50.Ct, 42.50.Ar

I. INTRODUCTION

Deterministic solid-state single-photon sources (S4Ps) are fundamental building blocks of potential quantum devices in the areas of quantum communication, cryptography,[1] and computation.[2] Each of these applications sets a number of stringent requirements for the S4P to fulfill, including an efficient collection of the emitted light, and highly nonclassical (sub-Poissonian) photon correlations. Besides, the eventual manipulation of the quantum information relies on two-photon interference and thus requires the photons to be prepared in a given (pure) quantum state: this typically calls for a suppression of the decohering interactions with the solid-state environment. A number of S4Ps have been demonstrated in recent years, based on the use of either vacancies,[3,4] molecules,[5–7] or mesoscopic heterostructures.[8–13] The latter, specifically consisting in semiconductor quantum dots (QDs), are particularly attractive due to the increasing degree of accuracy with which they can be embedded in (and coupled to) different kinds of optical microcavities (MCs).[14]

The requirement of generating indistinguishable photons translates into that of driving the emitter's time evolution in a coherent fashion from the ground state to the radiating state, within time scales shorter than those the decoherence acts on. In this respect, coherent-carrier control in semiconductor nanostructures, based on the use of ultrafast laser pulses, was proven to be a powerful technique.[15] The excitation of the system by optical means, however, brings about the practical problem of discriminating the outcoming photon from the incoming radiation. While more sophisticated approaches have been theoretically proposed,[16,17] the schemes so far applied at an experiment level rely on the energy relaxation the quantum emitter undergoes between the excitation and the emission processes. The incoherent nature of such evolution, and the resulting classical uncertainty on the starting time of the photon-emission process (time jitter), could render such schemes inherently inadequate to the implementation[17] of a S4P. It is the purpose of the present paper to gain a deeper insight into the above issue, and to show that, to a large extent, a full exploitation of the system engineering allows to circumvent such limitations.

The paper is organized as follows. In Sec. II, we describe the model and the theoretical framework we used to study the system's dynamics. Section III contains our results: we first present the no-dephasing case, where an empirical relationship between the indistinguishability and the collection efficiency is derived; we then analyze the effect of dephasing. The conclusions are finally drawn in Sec. IV.

II. THEORETICAL DESCRIPTION

The physical system we shall refer to in the following consists of a single semiconductor QD resonantly coupled to an optical MC. The discrete nature of the dot spectrum and the large interlevel spacings characterizing self-assembled QDs allow the selective addressing of its interband transitions by means of laser pulses at the ps time scale.[18] As a consequence, the system can be substantially prevented from being multiply excited, and its state vector effectively confined within a reduced portion of the Hilbert space. We accordingly restrict ourselves to a few QD states: the ground (or vacuum) state $|G\rangle$, the lowest exciton state $|X\rangle$, and the first excited state among the optically active ones $|X^*\rangle$. We consider a single cavity mode, with no *a priori* restriction on its occupation number n. The probability of a multiple-excitation ($n>1$, or $n>0$ with the QD in one of its exciton states) turns out to be negligible throughout the system's time evolution for the considered range of physical parameters: the level structure we shall refer to in the discussion of our results thus reduces to the one represented in Fig. 1.

In order to account for the open nature of the dot-cavity system, namely for its coupling with the phonon and the photon reservoirs, we describe the time evolution of the density operator ρ by means of the following master equation in the Lindblad form:

$$\dot{\rho} = \frac{i}{\hbar}[\rho, H] + \frac{\gamma}{2}\sum_{i=1}^{3}(2\mathbb{P}_i\rho\mathbb{P}_i - \mathbb{P}_i\rho - \rho\mathbb{P}_i) + \sum_{\alpha=r,s}\frac{\Gamma_\alpha}{2} \times (2\sigma_\alpha\rho\sigma_\alpha^\dagger - \sigma_\alpha^\dagger\sigma_\alpha\rho - \rho\sigma_\alpha^\dagger\sigma_\alpha) + \kappa(2a\rho a^\dagger - a^\dagger a\rho - \rho a^\dagger a), \quad (1)$$

where $\sigma_s = |G\rangle\langle X|$, $\sigma_r = |X\rangle\langle X^*|$, $\mathbb{P}_1 = |G\rangle\langle G|$, $\mathbb{P}_2 = |X\rangle\langle X|$, and

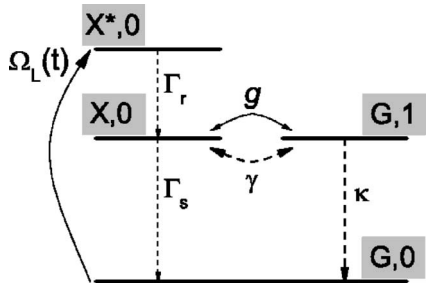

FIG. 1. Schematics of the dot-cavity system's relevant states: $|G,0\rangle, |G,1\rangle, |X,0\rangle, |X^*,0\rangle$. The occupation of the remaining states is negligible throughout the system's time evolution. In all the calculations presented below, we consider the case of a QD resonantly excited from $|G\rangle$ to $|X^*\rangle$ by means of a Gaussian laser pulse $\Omega_L(t)=\Omega_0 \exp[(t-t_0)^2/2\sigma^2]$, with $\sigma=1.1$ ps and $\Omega_0=0.75$ meV.

$\mathbb{P}_3=|X^*\rangle\langle X^*|$. The constant and time-dependent components of the Hamiltonian H, given by $H_{DC}=\hbar g(\sigma_s a^\dagger + a\sigma_s^\dagger)$ and $H_L=\hbar\Omega_L(t)(\sigma_r+\sigma_r^\dagger)$, account for the coherent couplings of the dot with the MC and with the driving laser, respectively.

Interference represents a natural means to measure the overlap between the quantum states of two photons consecutively emitted (one per driving pulse) by the single-photon source. Within a Hong-Ou-Mandel type experiment,[8,19] the indistinguishability is reflected by the bunching behavior of the two photons entering the two input channels of a balanced beam splitter. More specifically, a perfect overlap between the photons' state vectors completely suppresses the probability of measuring one photon in each of the two output channels. The experimentally accessible quantity accounting for such coincidence probability can be obtained from the emitter's first-order coherence functions[17,20]

$$p_c^\chi = \frac{\int_0^T dt \int_0^{T-t} d\tau [G_\chi^{(1)}(t)G_\chi^{(1)}(t+\tau) - |G_\chi^{(1)}(t,\tau)|^2]}{\int_0^T dt G_\chi^{(1)}(t) \int_0^{T-t} d\tau G_\chi^{(1)}(t+\tau)}, \quad (2)$$

where $G_{QD}^{(1)}(t,\tau)\equiv\langle\hat{\sigma}_s^\dagger(t)\hat{\sigma}_s(t+\tau)\rangle$, $G_{MC}^{(1)}(t,\tau)\equiv\langle\hat{a}^\dagger(t)\hat{a}(t+\tau)\rangle$, $G_\chi^{(1)}(t)\equiv G_\chi^{(1)}(t,0)$ ($\chi=MC,QD$); T is the time interval between two consecutive laser pulses, which we assume is larger than that the system requires to emit the photon and relax back to its ground state.

III. RESULTS

For the sake of clarity, we start by considering the photon properties in the absence of dephasing ($\gamma=0$). In Fig. 2(a)–2(d), we show the coincidence probabilities for the photons emitted by the QD and by the MC (p_c^{QD} and p_c^{MC}, respectively). Each symbol (square, circle, or triangle) corresponds to a given value of the Purcell factor, $F_p=2g^2/\kappa\Gamma_s$, i.e., to a specific ratio between the MC and QD emission rates; the overall rate emission $R=\Gamma_s+2g^2/\kappa$ increases along the horizontal axis from 0.01 to 1 times Γ_r, while either κ or g are kept constant [panels (a), (b) and (c), (d), respectively]. The photon indistinguishability clearly depends on the physical parameters solely through the overall-emission rate R normalized to Γ_r, while it is hardly affected by orders-of-magnitude changes in the Purcell factor. Moreover, such dependence is very well approximated by the simple expression

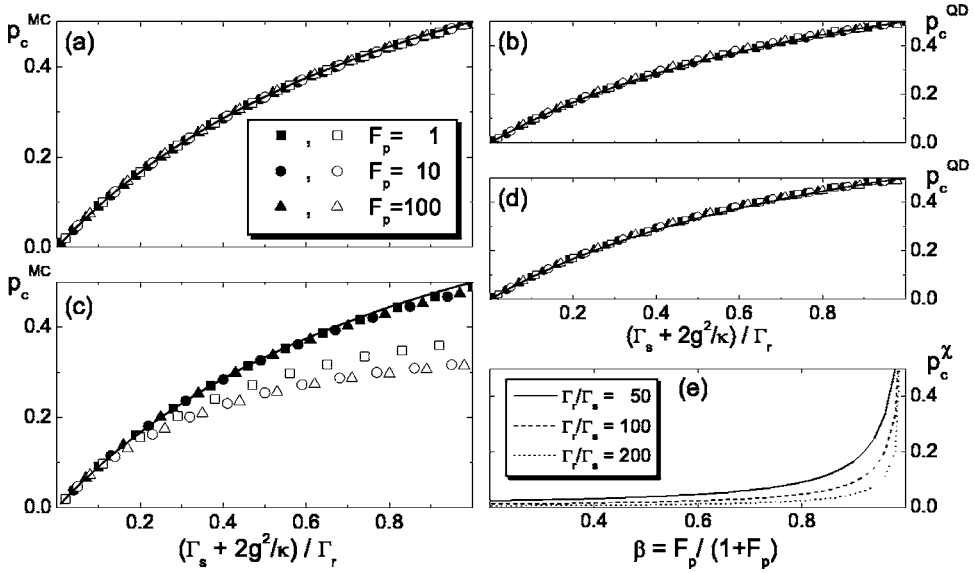

FIG. 2. (a)–(d) Distinguishability of the photons emitted by the microcavity (p_c^{MC}) and by the quantum dot (p_c^{QD}) as a function of the overall rate emission $R\equiv\Gamma_s+2g^2/\kappa$ normalized to Γ_r, in the absence of dephasing ($\gamma=0$). Different symbols stand for $F_p=1$ (squares), $F_p=10$ (circles), and $F_p=100$ (triangles). Solid lines depict the curve $p_c=R/(R+\Gamma_r)$. In each plot, Γ_s and either g [panels (c), (d)] or κ [(a), (b)] are varied in such a way that $\Gamma_s=R/(F_p+1)$ and $2g^2/\kappa=RF_p/(F_p+1)$. The fixed parameters are (a), (b) $\kappa=10$ ps^{-1}, $\Gamma_r=0.2$ ps^{-1} (black symbols), and 0.05 (white symbols); (c), (d) $\Gamma_r=0.1$ ps^{-1}, $g=0.2$ meV (black), and 0.05 (white). (e) Empirical relation between the collection efficiency β and p_c for different values of Γ_r/Γ_s.

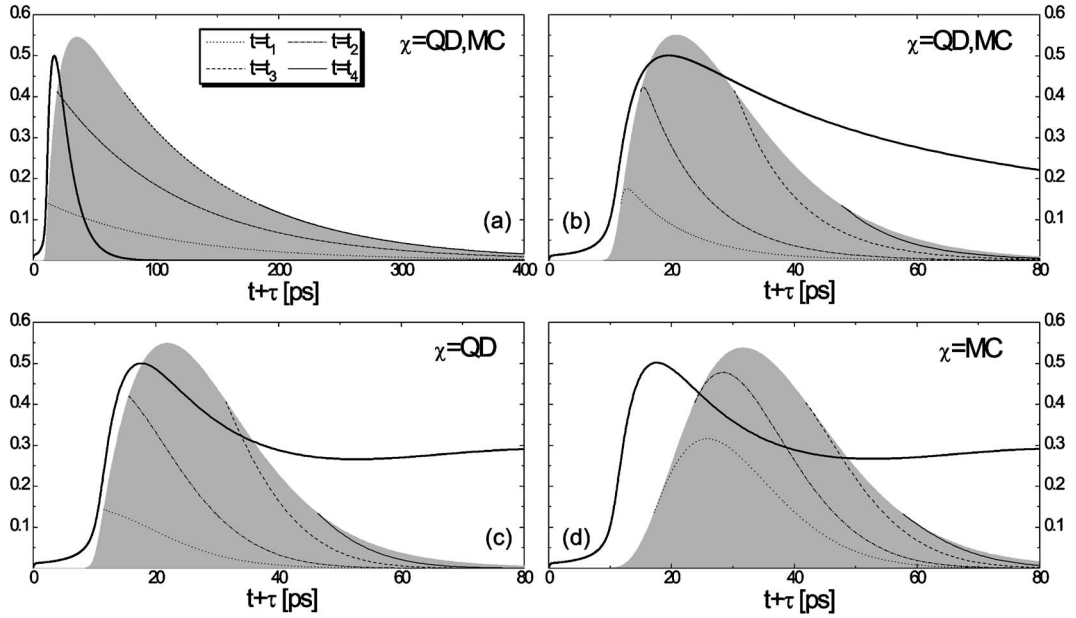

FIG. 3. Degree of purity and coherence of the dot-cavity system as a function of time. The purity (thick curves) is quantified by $f_{\tilde{\rho}}(t+\tau)\equiv 1-\mathrm{Tr}[\tilde{\rho}^2(t+\tau)]/\mathrm{Tr}[\tilde{\rho}(t+\tau)]^2$, calculated within the subspace $\{|G,1\rangle,|X,0\rangle,|X^*,0\rangle\}$. The coherence (narrow curves) is given by $|G_\chi^{(1)}(t,t+\tau)|^2/G_\chi^{(1)}(t)$, corresponding to different initial times $t=t_i$ and enveloped by $G_\chi^{(1)}(t+\tau)$ (shaded gray); the times t_i are such that $G_\chi^{(1)}(t_{2,3})=3G_\chi^{(1)}(t_{1,4})=0.75\ \max\{G_\chi^{(1)}(t)\}$. The labels on the vertical axes refer to $f_{\tilde{\rho}}$, while the other curves are plotted in arbitrary units. R/Γ_r is 1.0 in panel (a) and 0.1 in (b)–(d); g is 2.0 meV in panels (a), (b) and 0.05 in (c), (d); $\Gamma_r=0.1\ \mathrm{ps}^{-1}$ in (a)–(d).

$$p_c \equiv R/(R+\Gamma_r) \tag{3}$$

(solid curve in each of the panels), which is generally valid for both $\chi=QD$ and $\chi=MC$. This relationship holds as long as the only effect of the MC on the system's dynamics is that of enhancing the QD emission rate by a factor $(1+F_p)$, while it overestimates p_c^{MC} for $g\lesssim\Gamma_r,R$ [see panel (c) and the discussion below]. In fact, Eq. (3) can be analytically proven to be the exact solution, in the instantaneous-excitation limit, for the following simplified, three-level version of the system sketched in Fig. 1: in the case $g=0$, where the state $|G,1\rangle$ can be neglected. When such a three-level system is initialized to its highest state $|X^*,0\rangle$, the following equations hold:

$$\langle\sigma_r^\dagger(t)\sigma_r(t)\rangle=\Gamma_r(\mathrm{e}^{-\Gamma_r t}-\mathrm{e}^{-\Gamma_s t})/(\Gamma_s-\Gamma_r),$$

$$\langle\sigma_r^\dagger(t+\tau)\sigma_r(t)\rangle=\langle\sigma_r^\dagger(t)\sigma_r(t)\rangle\mathrm{e}^{-\Gamma_s\tau}. \tag{4}$$

The latter being a consequence of the quantum-regression theorem. After integrating and performing some algebra, Eq. (3) is derived for $R=\Gamma_s$.

Within a semiconductor-based S4P, the role of the MC is also that of meaningfully enhancing the collection efficiency.[21] In fact, the MC photons are typically emitted in one or a few well-defined directions, while the emission from the QD has a more isotropic character: the photon-loss probability can thus be approximately identified with that of the radiation being emitted directly by the QD into the leaky modes. Hereafter, we concentrate in the MC photon emission, for which we assume a maximum collection efficiency. The calculated fraction of photons emitted from the cavity is $\beta=N_{MC}/(N_{MC}+N_{QD})$, being $N_{MC}=2\kappa\int_0^T dt\langle a^\dagger(t)a(t)\rangle$, and $N_{QD}=\Gamma_s\int_0^T dt\langle\sigma_s^\dagger(t)\sigma_s(t)\rangle$. Within the considered range of physical parameters, the collection efficiency is readily expressed as a function of the Purcell factor:[21] $\beta=F_p/(F_p+1)=1-\Gamma_s/R$. The existence of simple and general expressions for both p_c^χ and β allows to establish between the two a relation which assigns to the ratio Γ_r/Γ_s a key role in the performance of the device

$$p_c=\left[1+\frac{\Gamma_r}{\Gamma_s}(1-\beta)\right]^{-1}. \tag{5}$$

While the degree of photon indistinguishability monotonically decreases with increasing collection efficiency [Fig. 2(e),[17] the possibility of contextually achieving for both β and $1-p_c$ values close to 1 sensitively depends on the ratio Γ_r/Γ_s and calls for its maximization. As discussed below, positive or negative corrections to such estimates of the coincidence probability may arise respectively from the presence of dephasing and from a proper weakening of the dot-cavity coupling.

A deeper physical insight into the above behaviors can be gained by looking at the time evolution of the populations $\rho_{\alpha,\alpha}$ and of the correlation functions. The narrow lines in Fig. 3 correspond to $|G_\chi^{(1)}(t,t+\tau)|^2/G_\chi^{(1)}(t)$, plotted as functions of τ and for different values of the initial times $t=t_i$; the shaded gray areas which envelope them give $G_\chi^{(1)}(t+\tau)$ and coincide with either $\rho_{X,0;X,0}$ or $\rho_{G,1;G,1}$ depending on χ being equal to QD or MC. In both cases, being the difference between the two proportional to the integrand functions of Eq. (2), the closer the black curves are to their gray envelope, the more the photons are indistinguishable. The thick lines in the plots,

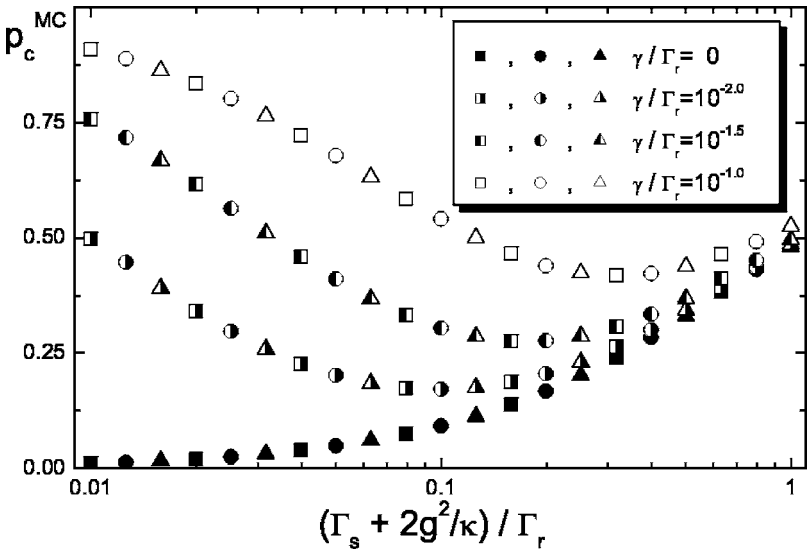

FIG. 4. Cavity-photon distinguishability as a function the rate emission R, for different values of the dephasing rate γ (see the legend) and of the Purcell factor F_p (squares, circles, and triangles correspond, respectively, to $F_p=1,10,100$). Other physical parameters: $\Gamma_r=0.1$ ps^{-1}, $g=0.2$ meV.

instead, quantify the degree of purity of the dot-cavity system, for they correspond to the function $f_{\tilde{\rho}}(t+\tau)\equiv 1-\mathrm{Tr}[\tilde{\rho}^2(t+\tau)]/\mathrm{Tr}[\tilde{\rho}(t+\tau)]^2$, with $\tilde{\rho}$ the density matrix reduced to the subspace $\{|G,1\rangle,|X,0\rangle,|X^*,0\rangle\}$. Quite generally, a large contribution to the value of p_c^X arises from the coherence functions whose initial time t_i falls in the raising region of $G_X^{(1)}$, while those with a later t_i tend to approach the envelope. The intuitive explanation for this feature is that the photon fraction emitted at any time t is not linearly superimposed to (and therefore does not interfere with) the contribution arising from the population of ρ which still has not undergone the energy relaxation, namely, $\rho_{X^*,0;X^*,0}(t)$. The comparison between the time evolutions corresponding to $R/\Gamma_r=0.1$ and $R/\Gamma_r=1.0$ [panels (a) and (b)] clearly shows how a slow emission strongly reduces the relative importance of the emission during the rising of $\rho_{X,0;X,0}$ and $\rho_{G1;G,1}$ and thus the average mixing of the system during the radiative process. The very same interpretation applies to the dependence of p_c^{MC} on the dot-cavity coupling constant g [Fig. 2(c)]. In fact, while for relatively large values of g, the population of the states $|X,0\rangle$ and $|G,1\rangle$ occurs simultaneously [Fig. 3(b)], for weaker dot-cavity couplings, the latter suffers a delay with respect to the former [panels (c), (d)]: the maximum of $\rho_{G1;G,1}$ is thus displaced with respect to that of $f_{\tilde{\rho}}$, and the photon emitted by the MC experiences on average a higher degree of purity with respect to that coming from the QD. Correspondingly, p_c^{MC} and p_c^{QD} coincide with p_c for $g>\Gamma_r,R$, while $p_c^{MC}<p_c^{QD}\simeq p_c$ for $g<\Gamma_r,R$. Thus, against intuition, a relative strengthening of the QD's incoherent interaction with the phonon reservoir (Γ_r) with respect to the coherent dot-cavity coupling (g) results in an increased degree of indistinguishability of the emitted photon, due to a deviation of the system's time evolution from that of the effective three-level system discussed to understand the simple expression (3).

Unlike atomic emitters, QDs are permanently coupled to a solid-state environment, which provides a number of scattering channels, mainly related to the lattice vibrations.[15,22] These include inelastic processes (real transitions), which are responsible for the nonradiative relaxation of the dot from $|X^*\rangle$ to $|X\rangle$, and elastic ones (virtual transitions), giving rise to the so-called pure dephasing. A detailed investigation of their physical origin and dependence on the specific features of the QD is beyond the scope of the present paper; in the following, we restrict ourselves to considering their effects on the properties of the emitted photons.

In Fig. 4, we show the coincidence probability p_c^{MC} as a function of the rate emission R, normalized to Γ_r, for different values of γ and of F_p. Once again, the key parameter turns out to be R, while no appreciable dependence on the Purcell factor shows up. On the other hand, a clear competition between γ and R emerges: the largest difference in the coincidence probabilities between the $\gamma\neq 0$ and the $\gamma=0$ cases occurs in the slow-emission region; the values of R at which the two values approach each other grow with increasing dephasing rate. However, the curves corresponding to different values of γ are not similar, i.e., they do not reveal any simple scaling behavior. We thus investigate the overall interplay between the relevant parameters, γ, Γ_r, and R, by considering the dependence of p_c^{MC} on the former two for fixed values of the latter (Fig. 5). For $R=0.101$ ps^{-1} [panel (a)], the photon indistinguishability is relatively unsensitive to the value of the dephasing rate, which is graphically rendered by the isolines being roughly parallel to the γ axis (see the left-hand side of the plot); instead, it meaningfully increases for increasing Γ_r. This indicates that already for $R/\gamma\gtrsim 10$ the requirement that the emission process be faster than dephasing is substantially satisfied, as suggested by the results of Fig. 4.While an order-of-magnitude reduction of the rate emission [panel (b)] invertes the above situation, the setting of R to 0.033 ps^{-1} [panel (c)] clearly enhances the area where $1-p_c^{MC}$ exceeds, 90%. Therefore, depending on which region of the (γ,Γ_r) plane can actually be accessed through the QD engineering and experimental conditions, the photon-emission rate needs to be either increased or decreased in order to improve the photon indistinguishability. Altogether, coincidence probabilities as low as 0.1 require an inelastic scattering rate Γ_r roughly two orders of magnitude larger than the elastic one γ, and a compromise value of R, such that $10\gamma\lesssim R\lesssim 0.1\Gamma_r$.

It should be mentioned that a fast, non-Markovian dephasing is known to affect the initial time evolution of the

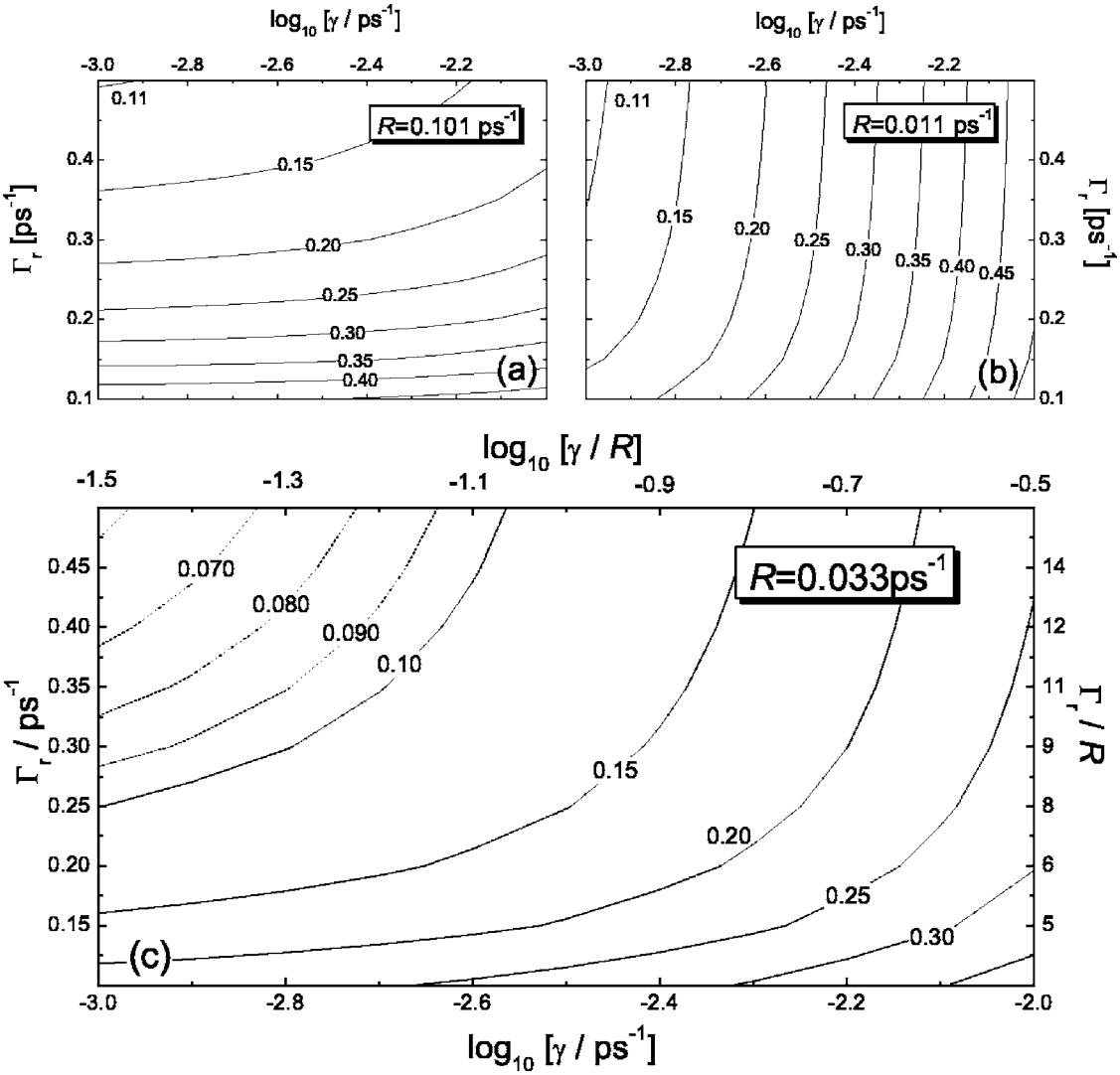

FIG. 5. Cavity-photon distinguishability as a function of the nonradiative relaxation and of the dephasing rates, Γ_r and γ, for different values of the rate emission R. In all cases $\Gamma_s = 10^{-3}$ ps^{-1}, while $F_p = 100, 10, 32$ in panels (a), (b), and (c), respectively. The dot-cavity coupling constant is $g = 0.1$ meV in (a), (b) and 0.05 in (c). The behavior of p_c^{MC} for $R = 0.033$ and $g = 0.1$ meV (not shown here) is qualitatively that shown in panel (c), though the values are on average higher.

dot polarization.[23,24] If analogous behaviors did apply to the dot-cavity structures of our present concern, the main effect might be an incomplete occupation of the $|X^*\rangle$ state, and thus a slightly reduced efficiency in the photon emission. The Markovian approach, however, would still be appropiate for the modeling of the subsequent, slow exponential dephasing.[23] Besides, the phonon spectrum, e.g., of a pillar microcavity is expected to dramatically differ from that of bulk, which is typically assumed in the derivation of the above non-Markovian behaviors; this makes its extension to the dot-cavity structures far from obvious.

IV. SUMMARY

In conclusion, the indistinguishability of the photons emitted by an incoherently excited dot-cavity system essentially depends on the relative efficiency of the system's nonradiative and radiative relaxations, i.e., on R/Γ_r. A simple empirical relation between such a ratio and the coincidence probability is found in the slow-dephasing limit; this in turn allows to express p_c as a function of β and to highlight the key role played by Γ_r/Γ_s within the device performance. The overall interplay between R, Γ_r, and the dephasing rate γ is investigated over a wide range of these parameters, providing indications for the design of QD-based single-photon sources.

ACKNOWLEDGMENTS

This work was partly supported by the Spanish MCyT under Contract No. MAT2002-00139, CAM under Contract No. 07N/0042/2002, and the EC within the Research Training Network COLLECT.

*Corresponding author. Email address: filippo.troiani@uam.es

[1] M. A. Nielsen and I. L. Chuang, *Quantum Computation and Quantum Information* (Cambridge University Press, Cambridge, England, 2000).
[2] E. Knill, R. Laflamme, and G. J. Milburn, Nature (London) **409**, 46 (2001).
[3] C. Kurtsiefer, S. Mayer, P. Zarda, and H. Weinfurter, Phys. Rev. Lett. **85**, 290 (2000).
[4] A. Beveratos, R. Brouri, T. Gacoin, J. P. Poizat, and P. Grangier, Phys. Rev. A **64**, 061802(R) (2001).
[5] F. De Martini, G. Di Giuseppe, and M. Marrocco, Phys. Rev. Lett. **76**, 900 (1996).
[6] C. Brunel, B. Lounis, P. Tamarat, and M. Orrit, Phys. Rev. Lett. **83**, 2722 (1999).
[7] B. Lounis and W. E. Moerner, Nature (London) **407**, 491 (2000).
[8] C. Santori, D. Fattal, J. Vukovic, G. S. Solomon, and Y. Yanamoto, Nature (London) **419**, 594 (2002).
[9] P. Michler, A. Kiraz, C. Becher, W. V. Schoenfeld, P. M. Petroff, L. Zang, E. Hu, and A. Imamoglu, Science **290**, 2282 (2000).
[10] C. Santori, M. Pelton, G. Solomon, Y. Dale, and Y. Yamamoto, Phys. Rev. Lett. **86**, 1502 (2001).
[11] V. Zwiller, H. Blom, P. Jonsson, N. Panev, S. Jeppesen, T. Tsegaye, E. Goobar, M. Pistol, L. Samuelson, and G. Bjrk, Appl. Phys. Lett. **78**, 2476 (2001).
[12] E. Moreau, I. Robert, J. M. Gérard, I. Abram, L. Manin, and V. Thierry-Mieg, Appl. Phys. Lett. **79**, 2865 (2001).
[13] Z. Yuan, B. E. Kardynal, R. M. Stevenson, A. J. Shields, C. J. Lobo, K. Cooper, N. S. Beattie, D. A. Ritchie, and M. Pepper, Science **295**, 102 (2002).
[14] A. Badolato, K. Hennessy, M. Atatüre, J. Dreiser, E. Hu, P. M. Petroff, and A. Immamoğlu, Science **308**, 1158 (2005).
[15] J. Shah, *Ultrafast Spectroscopy of Semiconductors and Semiconductor Nanostructures* (Springer, Berlin, 1999).
[16] C. K. Law and H. J. Kimble, J. Mod. Opt. **44**, 2067 (1997); A. Kuhn, M. Hennrich, T. Bondo, and G. Rempe, Appl. Phys. B: Lasers Opt. **B69**, 373 (1999).
[17] A. Kiraz, M. Atatüre, and A. Immaoğlu, Phys. Rev. A **69**, 032305 (2004).
[18] See., e.g., A. Zrenner, E. Beham, S. Stufler, F. Findeis, M. Bichler, and G. Abstreiter, Nature (London) **418**, 612 (2002), and references therein.
[19] C. K. Hong, Z. Y. Ou, and L. Mandel, Phys. Rev. Lett. **59**, 2044 (1987).
[20] J. I. Perea, D. Porras, and C. Tejedor, Phys. Rev. B **70**, 115304 (2004).
[21] J -M. Gerard, B. Gayral, and E. Moreau, quant-ph/0207115 (unpublished).
[22] F. Rossi and T. Kuhn, Rev. Mod. Phys. **74**, 895 (2002).
[23] P. Borri, W. Langbein, S. Schneider, U. Woggon, R. L. Sellin, D. Ouyang, and D. Bimberg, Phys. Rev. Lett. **87**, 157401 (2001).
[24] B. Krummheuer, V. M. Axt, and T. Kuhn, Phys. Rev. B **65**, 195313 (2002).